Polymer(Korea), Vol. 40, No. 3, pp. 355-364 (2016)
http://dx.doi.org/10.7317/pk.2016.40.3.355

ISSN 0379-153X(Print)
ISSN 2234-8077(Online)

Poly(ethylene-*co*-vinyl acetate), Polylactic Acid, 그리고 TiO_2 나노입자로 이루어진 나노복합소재의 제조 및 분석

Do Van Cong†, Nguyen Thi Thu Trang, Nguyen Vu Giang, Tran Huu Trung, Nguyen Thuy Chinh, Mai Duc Huynh, Thai Hoang†, and 박준서*,†
베트남과학원 열대기술연구소, *한경대학교 화학공학과
(2015년 9월 10일 접수, 2015년 12월 13일 수정, 2016년 1월 25일 채택)

Preparation and Characterization of Nanocomposites Based on Poly(ethylene-*co*-vinyl acetate), Polylactic Acid, and TiO_2 Nanoparticles

Do Van Cong†, Nguyen Thi Thu Trang, Nguyen Vu Giang, Tran Huu Trung, Nguyen Thuy Chinh, Mai Duc Huynh, Thai Hoang†, and Jun Seo Park*,†

Institute for Tropical Technology, Vietnam Academy of Science and Technology, 18 Hoang Quoc Viet, Cau Giay, Hanoi, Vietnam
**Department of Chemical Engineering, Hankyong National University, 67 Sukjong-dong, Ansung-city, Kyonggi-do 17579, Korea*
(Received September 10, 2015; Revised December 13, 2015; Accepted January 25, 2016)

Abstract: This study describes the preparation and characterization of nanocomposites obtained by melt-mixing of poly (ethylene-*co*-vinyl acetate) (EVA), polylactic acid (PLA), and TiO_2 nanoparticles (TNPs) via three different methods of direct mixing, one-step, and two-step methods. Vinyltrimethoxysilane was used as a surface modifier for the TNPs. The one-step method showed the best suitability for the preparation of EVA/PLA/TiO_2 nanocomposites. The increase in torque and the adhesion of the TNPs with EVA/PLA matrix in these nanocomposites showed enhanced interfacial interactions between EVA, PLA chains, and TNPs. The tensile strength, Young's modulus, dynamic storage modulus, and thermo-oxidative stability of the one-step prepared nanocomposites were higher than those of two other nanocomposites and that of the EVA/PLA blend, reaching maximum values at 2.0 wt% of TNPs.

Keywords: nanocomposites, polylactic acid, poly(ethylene-*co*-vinyl acetate), mixing, blend.

Introduction

The development of new polymeric materials by combining biodegradable polymers with non-biodegradable components is an interesting recent research trend that satisfies both environmental and application-specific requirements. Blends of the biodegradable polymer polylactic acid (PLA) and the synthetic non-biodegradable poly(ethylene-*co*-vinyl acetate) (EVA) have received increasing attention from scientists in recent years.[1-9] PLA and PLA-based materials are not only biodegradable but also produced from renewable natural resources, such as corn-starch and tapioca, and have the advantages of thermo-plasticity, high mechanical strength, and transparency.[8,10,11] EVA is a copolymer of ethylene and vinyl acetate units with many benefits of excellent flexibility, fracture toughness, light-transmission properties, good elongation at break, and good adhesion to both organic and inorganic materials.[12,13] Blending PLA with EVA utilizes the advantages of the two polymer components. In addition, some disadvantages of PLA, including brittleness, low elongation at break, high price, and low heat resistance,[8] and those of EVA, including low modulus and non-biodegradability,[12,13] can be overcome by compounding the materials. Ma *et al*.[5] showed that EVA increased the toughness of PLA. By introducing EVA into PLA, the elongation at break of the PLA/EVA blend was improved.[1,5] Blends containing above 50 wt% EVA had good elongation at break and are main subject of current studies on PLA/EVA blends.[5-9] However, high EVA contents decreased the tensile strength of PLA and strongly affected the thermal properties and degradation of PLA/EVA blends.[1,3-5,7] In these cases, fillers are added to

†To whom correspondence should be addressed.
E-mail: dovancongitt@itt.vast.vn; hoangth@itt.vast.vn; jspark@hknu.ac.kr

improve the properties of composite and promote degradation of polymer blend. However, few studies have been performed on ternary PLA/EVA-based composites with additive fillers. Recently, composites of PLA/EVA blends with black carbon powder and carbon nanotubes were studied.[14,15] The dispersion of these additives strongly affected the electrical resistivity of the composites. The effects of other additive fillers on other properties such as the mechanical, thermal, and biodegradable behaviors of the PLA/EVA blends have not yet been characterized.

TiO_2 is an attractive additive filler for chemical stability, biocompatibility, and optical and electrical properties of ceramic. It is widely used for environmental applications such as water and air disinfection.[16,17] TiO_2 nanoparticles (TNPs) with strong photo-catalytic activity have been introduced into various polymers such as polyethylene,[18] polypropylene,[19] polystyrene,[20] and poly(vinyl chloride)[21] to enhance the mechanical-thermal properties and promote decomposition of the obtained composites. The incorporation of TNPs into PLA has also gained much attention.[22-30] The tensile strength, Young's modulus, and degree of crystallinity of PLA/TiO_2 nanocomposites increased in the presence of TNPs.[25-27,29] TNPs also accelerated the hydrolysis, biodegradation, and photo-degradation of PLA.[25,27-30] In some recent studies, EVA/TiO_2 nanocomposites were studied.[31,32] Benito *et al.*[32] found that uniform dispersions of TNPs affected the coefficient of thermal expansion of EVA/TiO_2 nanocomposites. Generally, the preparation methods and interfacial phase interactions between TNPs and PLA and/or EVA have strong influences on the dispersibility of TNPs in the polymer and the properties of the nanocomposite. Solution casting is the most widely used method to prepare these nanocomposites.[22,24-26,29] In the latest studies, melt-mixing was used to prepare PLA/TNP and EVA/TNP composites.[30-33] The method is economically and environmentally friendly for the preparation of polymer nanocomposites and is the most promising and practical method for industrial use, since solvents are not required. To improve the dispersibility of TNPs in PLA matrix, different agents such as stearic acid,[22] propionic acid, *n*-hexylamine,[25] and L-lactic acid oligomer[26,30] have been used to modify TNP surfaces. However, TNPs modified by organic acid or *n*-hexylamine did not improve the tensile strength or thermal stability of PLA/TiO_2 nanocomposites.[22,25,26,30] By contrast, grafting L-lactic acid oligomers onto the surface of TNPs to form chemical linkages between the TNPs and PLA did improve the tensile strength of the obtained nanocomposites by 23.1% and 12.1% compared to neat PLA and PLA/unmodified TiO_2 nanocomposites, respectively.[26] Some silane compounds have also been used as coupling agents for both PLA/TiO_2 and EVA/TiO_2 nanocomposites. These exhibited highly efficient improvements of the interfacial interactions and bonding between PLA and/or EVA matrices and TNPs, causing clear improvements in the mechanical properties of the nanocomposites. Zhuang *et al.*[27] conducted the surface modification of TNPs by γ-methacryloxypropyltrimethoxysilane (MPS), followed by the *in-situ* polymerization of lactic acid in the presence of the MPS-modified TNPs to prepare PLA/TiO_2 nanocomposites. With the MPS modification, TNPs were dispersed uniformly in the PLA matrix. Therefore, the tensile strength, elongation at break, and Young's modulus of PLA/TiO_2 nanocomposites containing 3% modified TNPs were improved by 83.6, 6.73, and 129.4%, respectively, compared to those of neat PLA. By using vinyltriethoxysilane as a coupling agent, Wanxi *et al.*[31] showed an interfacial bonding layer between EVA and TNPs, increasing the tensile strength of EVA/TiO_2 nanocomposites by 28% compared to that of pristine EVA.

Although PLA/TiO_2 nanocomposites and EVA/TiO_2 nanocomposites have been studied, ternary EVA/PLA/TiO_2 nanocomposites have not yet been characterized. Thus, this work focuses on studying the influence of preparation methods and TNP contents on the characteristics including torque, mechanical-rheological properties, thermo-oxidative stability, and morphology of EVA/PLA/TiO_2 nanocomposites, using vinyltrimethoxysilane (VTMS) as a surface modifier for TNPs.

Experimental

Materials. EVA resin under trade name Hanwha EVA 1315 with content of 15% vinyl acetate, density d=0.93 g/cm^3, melting temperature 88 °C, melt flow index (MFI) 1.8 g/10 min (190 °C/2.16 kg), a commercial product of Hanwha Chemical company (South Korea). PLA pellets with a density of 1.24 g/cm^3, MFI of 10-30 g/10 min/190 °C/2.16 kg, M_n=110 KDa, and M_w/M_n=1.7 were purchased from Nature Works LLC (USA) under the trade name of Nature Works® PLA Polymer 2002D. TiO_2 of grade Aeroxide® P25 (purity 99.5%) with 21 nm average particle size and VTMS (purity 98%) were purchased from Sigma-Aldrich (Singapore). Dicumyl peroxide (DCP), a white powder, was supplied by Junsei Chemical Corporation (Japan). Absolute ethanol was used as a solvent. All chemicals were used as received, except PLA and EVA, which were dried in a vacuum oven at 60 °C for 12 h before use.

Surface Modification of TiO_2 Nanoparticles. Grafting of VTMS onto the surface of TNPs was performed by the reaction of the surface hydroxyl groups on TNPs with the VTMS, as described in detail in our previous work:[34] 1.0 g VTMS was dissolved in 100 mL ethanol to form a VTMS/ethanol solution under continuous magnetic stirring at 200 rpm. Then, 10.0 g original TNPs (o-TNPs), dried at 80 °C overnight in a vacuum oven, were mixed with the solution under vigorous stirring for 30 min. Concentrated acetic acid solution was slowly added dropwise into the mixture as a pH-controlling agent; the mixture was heated to 60 °C. This system was maintained at 60 °C for 8 h and the precipitate was obtained by filtration. The filtrate was washed thoroughly in ethanol to remove excess VTMS. Finally, the resulting solid was dried at 80 °C overnight in a vacuum oven to obtain the modified TNPs (m-TNPs). The content of VTMS grafted onto m-TNPs was about 1.10 wt%, as determined by thermogravimetric analysis (TGA).

Preparation of EVA/PLA/TiO_2 Nanocomposites. The preparation of EVA/PLA/TiO_2 nanocomposites was performed by melt-mixing in an internal mixer (HAAKE) at 170 °C and 50 rpm rotor speed for 5 min. EVA and PLA with a fixed composition ratio of 30/70 (w/w) and different amounts of TNPs (1.0-3.0 wt% compared to the total weight of EVA/PLA blend) were prepared with three different feeding methods, as follows:

One-step Method (1S): EVA, PLA, and a certain amount of o-TNPs (1.0-3.0 wt%) were mixed together. 0.5 wt% VTMS dissolved in 1.0 mL absolute ethanol was injected into the mixture, which was gently stirred manually. The mixture was placed in a vacuum oven preheated to 50 °C for 30 min to evaporate ethanol solvent. The dried obtained mixture was mixed in the internal mixer.

Two-step Method (2S): TNPs were modified by VTMS as mentioned in the previous section. EVA, PLA pellets, and specific amounts of m-TNPs were mixed together manually and then by the internal mixer.

Direct Melt-mixing Method (D): This method was performed using the same procedure as the two-step method, but m-TNPs were substituted with o-TNPs. After finishing the mixing process in the internal mixer, the molten mixture was quickly transferred and molded to sheets of ~1.0 mm thickness by a hot-pressure instrument (Toyoseiki, Japan). All samples are listed as described in Table 1.

Characterization of EVA/PLA/TiO_2 Nanocomposites. **Torque:** The torque of the mixture of EVA, PLA, and TNPs during the melt-mixing process was recorded by Polylab 3.1 software connected to the internal mixer (HAAKE).

Table 1. Sample Codes and Compositions

Sample	Composition (wt%)				
	EVA	PLA	m-TNPs	o-TNPs	VTMS
E70	70	30	-	-	-
D-T1	70	30	-	1.0	-
D-T2	70	30	-	2.0	-
D-T3	70	30	-	3.0	-
D-T4	70	30	-	4.0	-
1S-T0	70	30	-	0.0	0.5
1S-T1	70	30	-	1.0	0.5
1S-T2	70	30	-	2.0	0.5
1S-T3	70	30	-	3.0	0.5
1S-T4	70	30	-	4.0	0.5
2S-T1	70	30	1.0	-	-
2S-T2	70	30	2.0	-	-
2S-T3	70	30	3.0	-	-
2S-T4	70	30	4.0	-	-

Mechanical Properties: The tensile strength, elongation at break, and Young's modulus of the EVA/PLA blends and EVA/PLA/TiO_2 nanocomposites were determined by a Zwick instrument (Germany) according to the ASTM D638 standard. Each material was measured five times to obtain an average value.

Thermogravimetric Analysis (TGA): Thermogravimetric analysis (TGA) was used to evaluate the thermo-oxidative stability of PLA/EVA/TiO_2 nanocomposites, using a thermogravimetric analyzer DTG-60H (TGA/DTA) Shimadzu (Japan) in an ambient atmosphere, from 20 to 600 °C at 10 °C/min.

Thermo-oxidative Testing: The nanocomposite specimens were thermally aged in a convection air-circulating oven at 70 °C for 168 h. The decrease in the tensile strength, elongation at break, and Young's modulus of EVA/PLA/TiO_2 nanocomposites was used to determine the thermo-oxidative stability.

Rheological Measurements: Rheological measurements were performed in a rheometer (C-VOR model, Bohlin Rheometer, Bohlin Instrument Co., UK) equipped with a solid fixture system. The samples, measuring approximately 50 mm× 10 mm×1 mm, were oscillated at a very small strain of approx-

imately 5% with frequencies ranging from 0 to 5 Hz to determine the linear elastic characteristics of the blends and nanocomposites.

Field Emission Scanning Electron Microscopy (FESEM): The morphologies of EVA/PLA/TiO_2 nanocomposites were characterized by field-emission scanning electron microscopy (FESEM), using a Hitachi S-4800 machine (Japan). To observe the structural morphologies of the nanocomposites, FESEM images of the post-tensile-test fractured surfaces of the samples were taken to evaluate the dispersion and adhesion of TNPs in EVA/PLA blends.

Results and Discussion

Torque. Torque relates directly to the relative melt viscosity of EVA/PLA blends and EVA/PLA/TiO_2 nanocomposites during the mixing process. By observing the changes in torque, the reactions and interactions between the components present in the blend and nanocomposites can be evaluated.

Figure 1 depicts the torque curves of EVA/PLA blend (E70) and EVA/PLA/TiO_2 nanocomposite containing 2 wt% TNPs prepared by the direct-mixing (D-T2), one-step (1S-T2), and two-step (2S-T2) methods. At the beginning of processing, the torque of the above samples increases to a maximum due to the addition of the materials into the mixing chamber. It is decreased as EVA and PLA begin plasticizing and melting. From 4 to 5 min of mixing, the torque of E70 sample remains nearly constant because then EVA and PLA are completely plasticized and melted, and the obtained torque is designated the stable torque. A similar phenomenon is observed for the torque changes of D-T2 and 2S-T2 samples. Interestingly, the stable torques of these samples are higher than that of E70 sample because the incorporation of TNPs obstructs molecular motion and decreases the mobility of PLA and EVA macromolecular chains. The torque of 2S-T2 sample is slightly increased in comparison to that of D-T2 sample because the VTMS modification of TNPs improves the compatibility and adhesion between m-TNPs and EVA/PLA blend. The silanol groups formed by hydrolysis of VTMS in the presence of the moisture (Scheme 1) and hydroxyl groups on the TNP surfaces can interact with the active polar groups in PLA and EVA macromolecular chains (e.g., carbonyl groups) by hydrogen bonding and dipole-dipole interactions, similar to the interactions between PLA chains and nanoclays.[35] Vinyl groups of VTMS on the m-TNPs (Scheme 1) are compatible with hydrocarbon segments of EVA and PLA chains. In addition, they can also attach to EVA and PLA chains by a grafting reaction which catalyzed by free radicals generated during mixing at high temperatures (Scheme 2 and 3).[31,36] For 1S-T2 sample, the torque increases dramatically from 2.2 to 5 min in the mixing process. After 5 min mixing, the torque of 1S-T2 sample is noticeably higher than that of both 2S-T2 and D-T2 samples. The *in-situ* formation of crosslinks between silanol groups formed by the hydrolysis of VTMS, the condensing reactions between silanol groups and hydroxyl groups on the surface of TNPs (Scheme 1), the grafting reaction of VTMS into EVA and PLA macromolecular chains (Scheme 2 and 3), and condensing reactions between silanol groups grafted on EVA and PLA (Scheme 4) might cause this increase in the torque of this

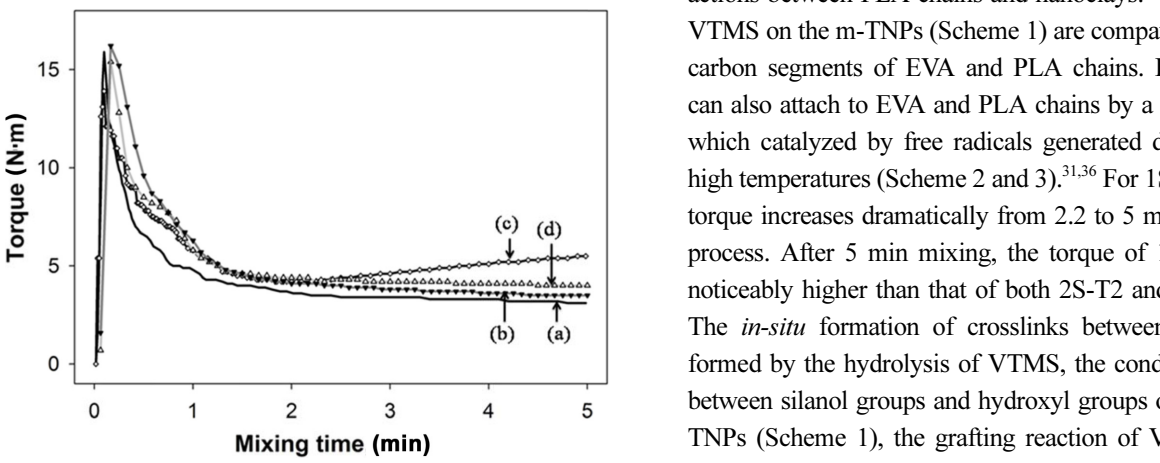

Figure 1. Torque curves *versus* mixing time of (a) EVA/PLA blend and nanocomposites containing 2.0 wt% TNPs prepared by (b) direct-mixing; (c) one-step method; (d) two-step method.

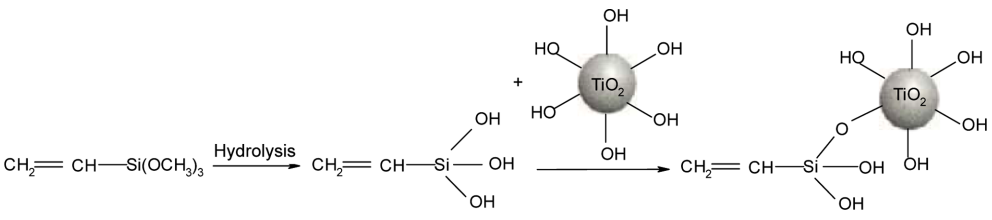

Scheme 1. Modification of TNPs surface by VTMS.

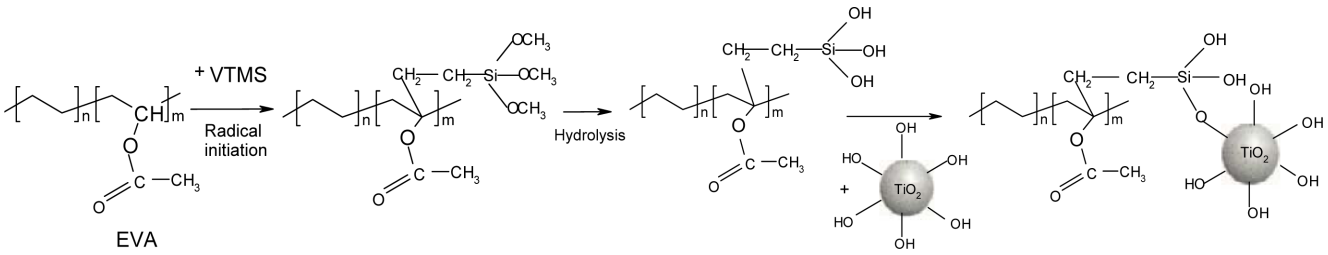

Scheme 2. Graft of VTMS on EVA chains, and bonding between VTMS-*g*-EVA and TNPs.

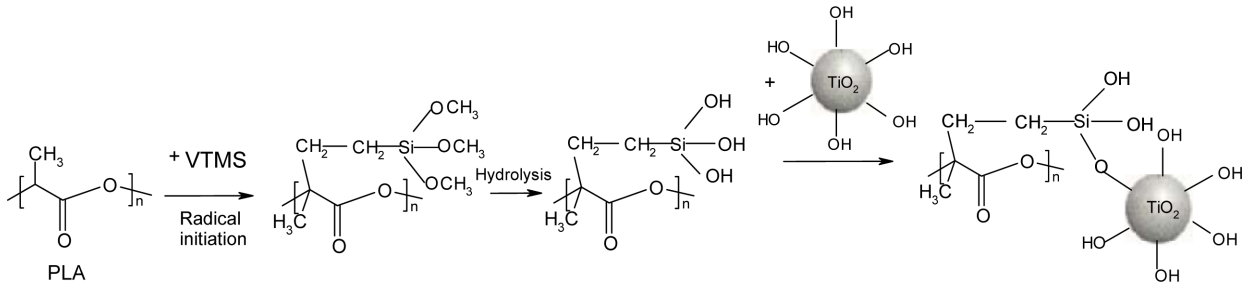

Scheme 3. Graft of VTMS on PLA chains, and bonding between VTMS-*g*-PLA and TNPs.

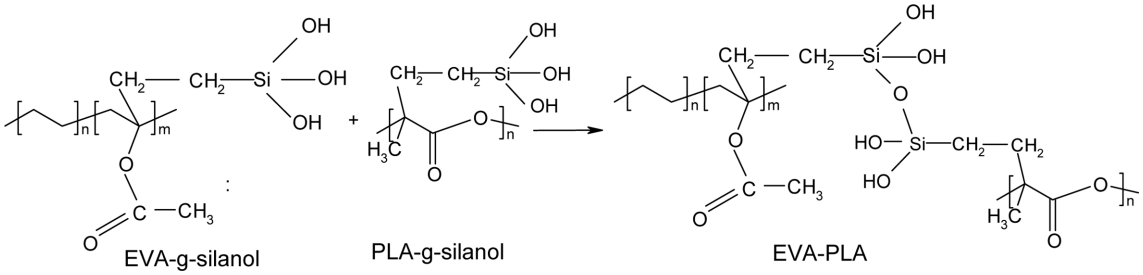

Scheme 4. Condensing reaction between silanol grafted on EVA and PLA chains.

sample.[31,36,37] Varghese *et al*.[38] and Mohamad *et al*.[39] confirmed that the increase of torque could result from high compatibility and good interactions between components in a molten mixture. With these reactions and interactions, the adhesion and compatibility between EVA, PLA macromolecular chains and TNPs in 1S-T2 nanocomposite were enhanced.

Figure 2 displays the torque curves of EVA/PLA blend and the one-step prepared nanocomposites (1S-nanocomposites) containing 0-4.0 wt% of TNPs. The shapes of the torque curves of all 1S-nanocomposites are similar but the torque values of these nanocomposites obtained after 5 min mixing increase gradually with increasing TNPs content (Table 2). The higher level of the obstacle and entanglement against the movement and mobility of EVA, PLA chains with rising TNPs content caused this increase. For 1S-T0 sample without TNPs, the grafting VTMS into EVA and PLA chains and the condensing reactions between silanol groups improved the compatibility and interactions between the PLA and EVA macromolecular chains, therefore increased slightly the torque value of 1S-T0 sample in comparison to that of E70 sample.

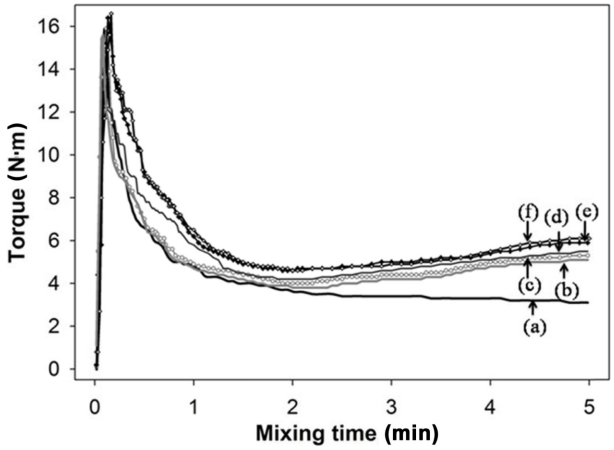

Figure 2. Torque curves of (a) EVA/PLA blend and 1S-nanocomposites containing TNPs contents of (b) 0; (c) 1.0; (d) 2.0; (e) 3.0; (f) 4.0 wt%.

Table 2. Torque Value of EVA/PLA Blend and 1S-Nanocomposites After 5 min of Mixing

Sample	E70	1S-T0	1S-T1	1S-T2	1S-T3	1S-T4
Torque (N.m)	3.1	5.1	5.3	5.5	5.9	6.1

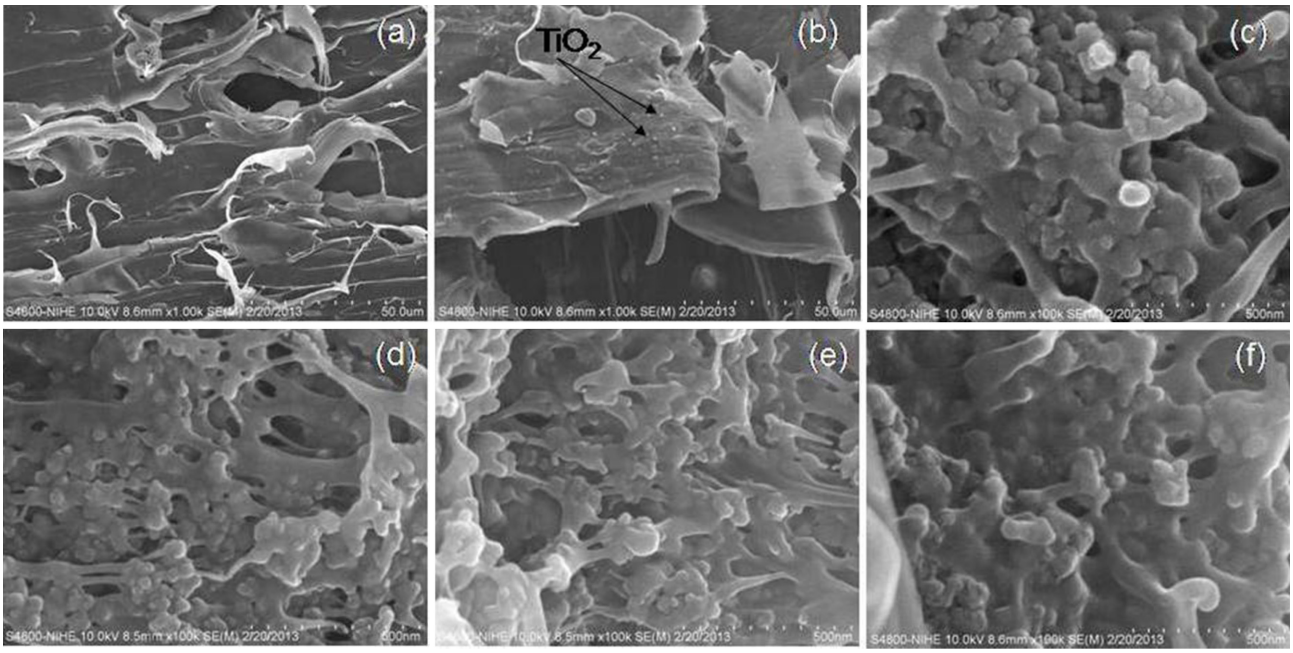

Figure 3. FESEM images of the tensile fractured surfaces of (a) EVA/PLA blends; (b) one-step prepared nanocomposites containing 2.0 wt% TNPs at the same magnification of 1 K×; (c, d, e) D-T2, 1S-T2, and 2S-T2 nanocomposites, respectively, containing 2.0 wt% TNPs at the magnification of 100 K×; (f) 1S-T3 nanocomposites containing 3.0 wt% TNPs at the magnification of 100 K×.

Morphology. To investigate the dispersions and adhesion of TNPs in EVA/PLA blends, FESEM analysis was performed on the tensile-fractured surfaces of the samples. Figure 3 demonstrates the FESEM images of the fractured surfaces of E70 blend and EVA/PLA/TiO_2 nanocomposites. Figure 3(a) shows that EVA and PLA phases are dispersed uniformly with each other; no TiO_2 particles appear in EVA/PLA blend. However, small white spots appear in the images of the fractured surface of EVA/PLA/TiO_2 sample shown in Figure 3(b) indicating that TiO_2 particles are dispersed in EVA/PLA blend by melt mixing. Figure 3(c), (d), and (e) depict the fractured surface images of nanocomposites containing 2.0 wt% TNPs prepared by D, 1S, and 2S methods, respectively. Here we observe the local dispersion of TNPs with particle sizes of 40-80 nm in EVA/PLA blend in D-nanocomposite. However, poor adhesion is observed between the TNPs and EVA and PLA. Some TNPs have agglomerated to form clusters of 100-150 nm in size. Meanwhile, relatively uniform dispersion and good adhesion between TNPs and EVA/PLA blends are observed in the 1S- and 2S-nanocomposites. In these, the TiO_2 particle size is ~20-40 nm. Clearly, the presence of VTMS as a surface modifier is important in enhancing the dispersibility, compatibility, and adhesion of TNPs with EVA/PLA blend. For 1S-nanocomposite containing 3.0 wt% TNPs, the dispersion of TNPs becomes more irregular and the particles begin to agglomerate in the blend, forming clusters of ~60-100 nm in size (Figure 3(f)).

Tensile Properties. Table 3 shows the Young's modulus (E_Y), tensile strength (σ), and elongation at break (ε) of E70 blend and EVA/PLA/TiO_2 nanocomposites prepared by the D, 1S, and 2S methods. E_Y of all nanocomposites is higher compared with that of E70 blend and increases with increasing TNP contents. At the same loading TNPs content, in ascending order; σ increases as D-nanocomposites < E70 < 2S-nanocomposites < 1S-nanocomposites. While, ε for the nanocomposites is lower than that of E70 blend and decreases with increasing TNP contents. The σ and ε of all D-nanocomposites are reduced in comparison with those of E70 sample. This indicates the incompatibility of EVA, PLA, and TNPs in these samples, leading to the formation of micro-defects; therefore,

Table 3. Young's Modulus (E_Y), Tensile Strength (σ) and Elongation at Break (ε) of EVA/PLA Blend and EVA/PLA/TiO_2 Nanocomposites

Sample	E_Y (MPa)	σ (MPa)	ε (%)
E70	184.20	7.95	234.35
1S-T0	198.68	9.13	198.27
1S-T1	221.55	10.14	149.23
1S-T2	222.19	11.49	143.59
1S-T3	224.84	9.74	95.62
1S-T4	225.72	9.31	81.75
2S-T1	220.95	9.72	186.63
2S-T2	221.86	10.20	156.13
2S-T3	221.95	9.95	86.63
2S-T4	222.14	9.12	73.22
D-T1	208.63	7.91	158.56
D-T2	211.27	7.34	92.44
D-T3	214.35	5.92	58.55
D-T4	215.41	5.31	42.10

the tensile properties of the obtained composites are weakened. σ of all 1S- and 2S-nanocomposites exceed that of EVA/PLA blend and increases with increasing the TNPs contents. The highest σ value occurs at 2.0 wt% TNPs content. At this level, σ of 2S- and 1S-nanocomposites is 28.3% and 44.5% greater, respectively, than that of the E70 blend. These values are higher by 17.1% than that of EVA/TiO_2 nanocomposites using vinyltriethoxysilane as a coupling agent[31] and by 28.0% than that of PLA/TiO_2 nanocomposites using the L-lactic acid oligomer to modify the TNPs.[26] The presence of VTMS clearly enhances the interfacial interactions and linkages between PLA, EVA chains, and TNPs as mentioned in section 3.1, resulting in these improvements. At TNP contents exceeding 2.0 wt%, σ for both 1S- and 2S-nanocomposites decreases because of TNP agglomeration, leading to form micro-defects in the nanocomposites. 1S-nanocomposites show the highest tensile properties among the tested nanocomposites because of the better dispersibility of TNPs in EVA/PLA blend and the improved compatibility and adhesion between the components in the nanocomposites, as mentioned previously.

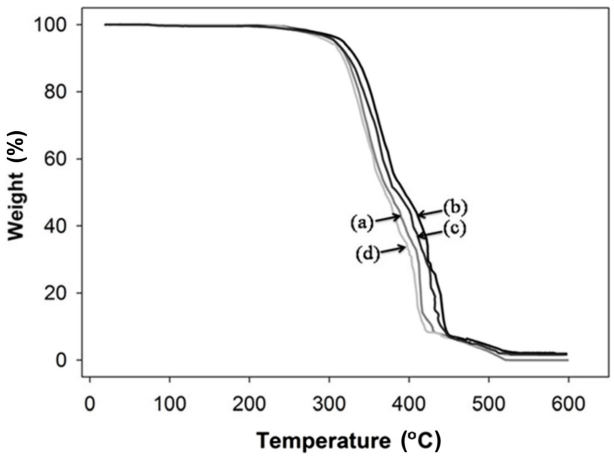

Figure 4. TG curves of (a) EVA/PLA blend and the nanocomposites containing 2.0 wt% TNPs prepared by (b) one-step method (1S-T2); (c) two-step method (2S-T2); (d) direct-mixing (D-T2).

Thermo-oxidative Stability. The thermo-oxidative stability of EVA/PLA/TiO_2 nanocomposites was assessed by TGA. Figure 4 presents the TG curves of E70 blend and EVA/PLA/TiO_2 nanocomposites containing 2.0 wt% TNPs prepared by the three methods. All TG curves show two stages of thermal degradation, indicated by two different slope stages. The first stage, from 260 to 380 °C, is assigned to the thermo-oxidative degradation of PLA[40] and the vinyl acetate (VA) segments in EVA. The latter, from 380 to 600 °C, relates to the thermo-oxidative degradation of hydrocarbon segments in EVA.[41]

The slopes of the TG curves of the samples rank in the order of 1S-T2 nanocomposite < 2S-T2 nanocomposite < E70 blend < D-T2 nanocomposite. The thermal characteristics obtained from the TG curves expressed in Table 4, indicate that the onset temperature of decomposition (T_d) and the remaining weight (W_r) of 1S-T2 and 2S-T2 nanocomposites at the same heating temperature exceed those of E70 blend and D-T2

Table 4. TG Characteristics of EVA/PLA Blend and EVA/PLA/TiO_2Nanocomposites Containing 2.0 wt% TNPs Prepared by One-step Method (1S-T2) and Two-step Method (2S-T2) and Direct Method (D-T2)

Samples	Onset temperature of decomposition, T_d (°C)	Remaining weight at the different temperatures, W_r (%)			
		350 °C	420 °C	460 °C	500 °C
E70	261.2	66.51	14.00	5.90	2.22
D-T2	260.4	64.51	9.34	5.82	2.03
2S-T2	266.5	75.27	29.55	6.24	2.30
1S-T2	271.4	80.49	36.48	6.85	4.54

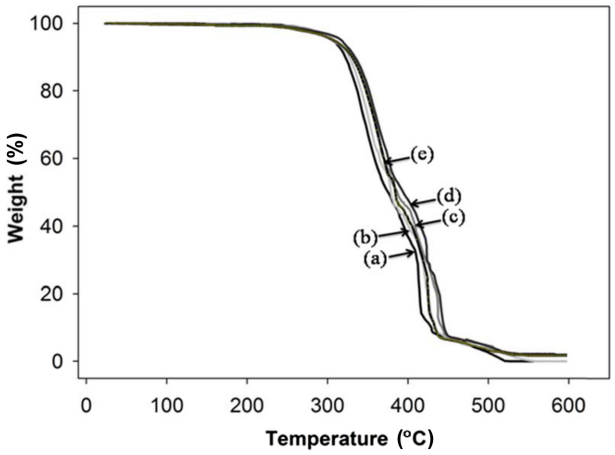

Figure 5. TG curves of (a) EVA/PLA and 1S-nanocomposites containing (b) 0; (c) 1.0; (d) 2.0; (e) 3.0 wt% TNPs.

nanocomposite. These results reveal that 1S-T2 and 2S-T2 samples have greater thermo-oxidative stability than D-T2 and E70 samples. The finer structure of 1S-T2 and 2S-T2 nanocomposites, as mentioned in section 3.2, limits the penetration of oxygen gas into these nanocomposites, thus reducing the thermo-oxidative degradation of EVA and PLA. These results also confirm that the addition of o-TNPs without surface modifications or the presence of VTMS reduces the thermo-oxidative stability of EVA/PLA blend.

TG curves of E70 blend and 1S-nanocomposites containing different TNPs contents are performed in Figure 5. The TG curves of all nanocomposites are located above the curve of E70 blend; the slopes decrease with increasing the TNPs contents from 0 to 2.0 wt%.

Table 5 represents the TG characteristics of E70 blend and 1S-nanocomposites containing different TNPs contents. From 1.0 to 2.0 wt% TNPs, T_d and W_r of the 1S-nanocomposites increase with increasing TNPs contents. The thermo-oxidative stability of 1S-nanocomposites is clearly improved at this level of TNPs content. The highest degree of improvement in the thermo-oxidative stability of the nanocomposites is found at 2.0 wt% of TNPs, with the highest T_d and W_r and the lowest TG slope. When the content of TNPs reaches 3.0 wt%, the slope of the TG curve of 1S-T3 nanocomposite increases and the T_d and W_r lower than those of 1S-T2 nanocomposite. This indicates that the thermo-oxidative stability of 1S-nanocomposites decreases when the content of TiO_2 reaches or exceeds 3.0 wt%, because the agglomeration of TNPs causes the formation of defects which accelerate the thermo-oxidative degradation of the nanocomposites as afore mentioned.

The thermo-oxidative stability of EVA/PLA/TiO_2 nanocomposites was also evaluated by thermo-oxidative testing in the convection air-circulating oven at 70 °C for 168 h. Table 6 lists the tensile properties and retention percentage of E70 blend and EVA/PLA/TiO_2 nanocomposites after thermo-oxidative aging. Compared to the tensile properties in Table 3, E_Y, σ, and ε for all samples decrease after 168 h aging. Among the tensile properties, ε seems the most sensitive to thermo-oxidative aging, with a higher degree of reduction compared to those of σ and E_Y. The changes in the tensile properties of aged 1S- and 2S-nanocomposites are not as severe as those in E70 blend. The retention percentage of tensile properties of D-nanocomposites is even smaller than that of the blend. This indicates that the thermo-oxidative stability of D-nanocomposites is not improved with the addition of o-TNPs. Among the tested nanocomposites, the reduction in tensile properties of 1S-nanocomposites is the smallest. At 2.0 wt% TNPs, the retention of tensile properties in both 1S- and 2S-nanocomposites is higher than those of the nanocomposites containing 1.0, 3.0, and 4.0 wt% TNPs. This demonstrates that thermo-oxidative stability of the nanocomposites is highest at 2.0 wt% TNPs. These results are similar to those obtained from the TG results.

Rheological Properties. Figure 6 shows the dependence of the dynamic storage modulus (E') on the frequency (f) of deformation for E70 blend and EVA/PLA/TiO_2 nanocomposites prepared by the three methods. The E' values of all samples increases with increasing f. With 2.0 wt% TNPs content, the E' values of all nanocomposites are higher than that of the blend. It indicates the incorporation of TNPs increases the

Table 5. TG Characteristics of E70 Blend and 1S-Nanocomposites Containing 1.0-3.0 wt% TNPs

Samples	Onset temperature of decomposition, T_d (°C)	Remaining weight at the different temperatures, W_r (%)			
		350 °C	420 °C	460 °C	500 °C
E70	261.2	66.51	14.00	5.90	2.52
1S-T0	266.4	76.34	26.07	6.14	3.70
1S-T1	269.5	80.32	31.50	6.64	4.51
1S-T2	271.4	80.49	36.48	6.85	4.54
1S-T3	267.7	76.95	29.76	6.03	3.38

Table 6. Tensile Properties of EVA/PLA Blend and EVA/PLA/TiO_2 Nanocomposites Before and After Thermo-oxidative Testing

Samples	E_Y (MPa)		σ (MPa)		ε (%)	
	After testing	% Retention	After testing	% Retention	After testing	% Retention
E70	162.76	88.36	6.87	86.42	193.95	82.76
1S-T0	185.17	93.20	8.41	92.11	178.78	90.17
1S-T1	213.84	96.52	9.78	96.45	139.93	93.77
1S-T2	218.61	98.39	11.32	98.52	135.84	94.60
1S-T3	216.88	96.46	9.29	95.38	87.18	91.17
1S-T4	212.63	94.20	8.72	93.66	72.23	88.35
2S-T1	211.76	95.84	9.15	94.14	172.09	92.21
2S-T2	216.85	97.74	9.85	96.57	147.01	94.16
2S-T3	207.86	93.65	9.22	92.66	78.26	90.34
2S-T4	204.10	91.88	8.21	90.02	63.79	87.12
D-T1	201.32	96.50	6.79	85.84	130.24	82.14
D-T2	199.37	94.37	6.22	84.74	75.11	81.25
D-T3	197.24	92.02	4.95	83.61	44.53	76.05
D-T4	194.56	90.32	4.33	81.54	30.31	72.00

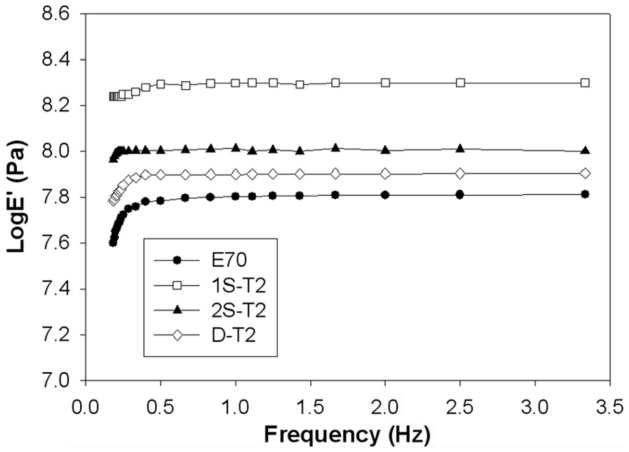

Figure 6. Dynamic storage modulus (E') of EVA/PLA blend (E70) and EVA/PLA/TiO_2 nanocomposites containing 2.0 wt% TNPs prepared by different methods.

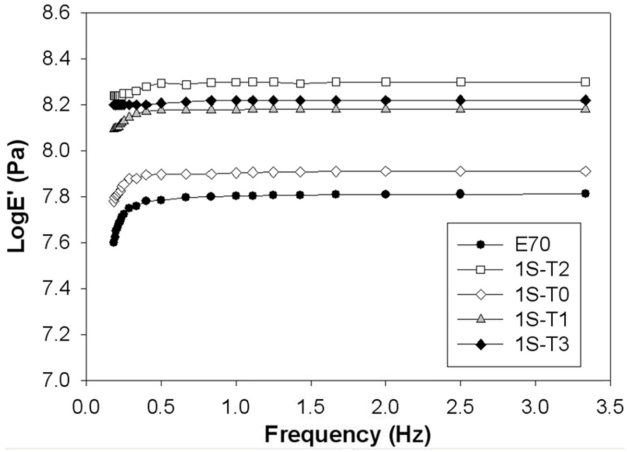

Figure 7. Dynamic storage modulus (E') of 1S-nanocomposites containing 0-3.0 wt% TNPs.

stiffness of EVA/PLA blend due to the obstacle and entanglement against the movement and mobility of EVA and PLA chains. The E' values of the nanocomposites are ranked in the following order: D-T2 < 2S-T2 < 1S-T2. It is due to the stronger interactions and the bonding formation between TNPs and EVA/PLA blend with the presence of VTMS as mentioned in the previous sections. The highest E' value of 1S-T2 nanocomposite compared to those of D-T2 and 2S-T2 nanocomposite shows the highest improvement in compatibility and adhesion of the components this nanocomposite.

Figure 7 presents the dependence of E' on TNPs content of the 1S-nanocomposites. As the TNPs contents do not exceed 2.0 wt%, the E' values of the nanocomposites increases with increasing f and TNPs content. It shows that the incorporation of TNPs increases the rigidity of EVA/PLA/TiO_2 nanocomposites and makes them exhibit more solid-like behavior. The E' values reach a maximum at 2.0 wt% TNPs. In this content, the improvement in the dispersibility, interactions and adhesion of the TNPs with EVA/PLA blend is the highest level, therefore, E' increases. However, when the content of TNPs increases to 3.0 wt%, E' of the 1S-nanocomposites decreases. This is because the structure of the composite becomes more heterogeneous with more TNPs. The aggregation of TNPs

occurs, forming defects in the nanocomposite structures and reducing E'.

Conclusions

EVA/PLA/TiO_2 nanocomposites were prepared by direct-mixing, a one-step method, and a two-step method. The highest values of tensile strength, Young's modulus, dynamic storage modulus, and thermo-oxidative stability demonstrated that the one-step method was the most suitable for the preparation of EVA/PLA/TiO_2 nanocomposites. In these nanocomposites, the interfacial interaction and dispersibility of TNPs in the EVA/PLA matrices were enhanced. The presence of VTMS was important in improving the compatibility, adhesion, and dispersibility of the components in EVA/PLA/TiO_2 nanocomposites. The TNPs contents also influenced the characteristics of the nanocomposites. The tensile strength, dynamic storage modulus, and thermo-oxidative stability of the nanocomposites were the highest with 2.0 wt% TNPs. At this level, the dispersion of TNPs in the EVA/PLA blend was fine and uniform.

Acknowledgments: This research is funded by the Vietnam National Foundation for Science and Technology Development (NAFOSTED) under grant number 104.04-2012.07.

References

1. J. S. Yoon, S. H. Oh, M. N. Kim, I. J. Chin, and Y. H. Kim, *Polymer*, **40**, 2303 (1999).
2. X. Liu, L. Lei, J. W. Hou, M. F. Tang, S. R. Guo, Z. M. Wang, and K. M. Chen, *J. Mater. Sci. M*., **22**, 327 (2011).
3. A. M. Gajria, V. Dave, R. A. Gross, and S. P. McCarthy, *Polymer*, **37**, 437 (1996).
4. D. V. Cong, T. Hoang, N. V. Giang, N. T. Ha, T. D. Lam, and M. Sumita, *Mat. Sci. Eng. C Mater*., **32**, 558 (2012).
5. P. Ma, D. G. Hristova-Bogaerds, J. G. P. Goossens, A. B. Spoelstra, Y. Zhang, and P. J. Lemstra, *Eur. Polym. J*., **48**, 146 (2012).
6. I. Moura, R. Nogueira, V. B. Legare, and A. V. Machado, *Mater. Chem. Phys*., **134**, 103 (2012).
7. H. M. Said and J. Radiat, *Res. Appl. Sci.*, **6**, 11 (2013).
8. P. Ma, P. Xu, W. Liu, Y. Zhai, W. Dong, Y. Zhang, and M. Chen, *RSC Adv*., **5**, 15962 (2015).
9. I. Moura, G. Botelho, and A. V. Machado, *J. Polym. Environ*., **22**, 148 (2014).
10. M. Farhoodi, S. Dadashi, S. M. A. Mousavi, R. S. Gharebagh, Z. E. Djomeh, A. Oromiehie, and F. Hemmati, *Polym. Korea*, **36**, 745 (2012).
11. L. J. Hun, L. Y. Hui, L. D. Sung, L. Y. Kwan, and N. J. Do, *Polym. Korea*, **29**, 375 (2010).
12. J. Jin, S. Chen, and J. Zhan, *Polym. Degrad. Stab*., **95**, 725 (2010).
13. G. H. Han, H. J. Shin, E. S. Kim, S. J. Chae, J. Y. Choi, and Y. H. Lee, *Nano*, **6**, 59 (2011).
14. Y. Y. Shi, J. H. Yang, T. Huang, N. Zhang, C. Chen, and Y. Wang, *Composites: Part B*, **55**, 463 (2013).
15. A. Katada, Y. F. Buys, Y. Tominaga, S. Asai, and M. Sumita, *Colloid Polym. Sci*., **284**, 134 (2005).
16. R. Vijayalakshmi and V. Rajendran, *Arch. Appl. Sci. Res*., **4**, 1183 (2012).
17. K. Zhang, X. Wang, X. Guo, J. Dai, and J. Xiang, *Nano*, **10**, 1550001 (2015).
18. F. Bondioli, A. Dorigato, P. Fabbri, M. Messori, and A. Pegoretti, *Polym. Eng. Sci*., **48**, 448 (2008).
19. N. S. Kwon and N. J. Woon, *Polym. Korea*, **30**, 397 (2006).
20. A. Zohrevand, A. Ajji, and F. Mighri, *Polym. Eng. Sci*., **54**, 874 (2014).
21. S. Cashmore, A. Robinson, and D. Worsley, *ECS Trans*., **25**, 95 (2010).
22. N. Fukuda and H. Tsuji, *J. Appl. Polym. Sci*., **96**, 190 (2005).
23. M. Song, C. Pan, J. Li, X. Wang, and Z. Gu, *Electroanalysis*, **18**, 1995 (2006).
24. C. Chen, G. Lv, C. Pan, and M. Song, *Biomed. Mater.*, **2**, L1 (2007).
25. N. Nakayama and T. Hayashi, *Polym. Degrad. Stab*., **92**, 1255 (2007).
26. X. Lu, X. Lv, Z. Sun, and Y. Zheng, *Eur. Polym. J*., **44**, 2476 (2008).
27. W. Zhuang, J. Liu, J. H. Zhang, B. X. Hu, and J. Shen, *Polym. Compos*., **30**, 1074 (2009).
28. J. O Carneiro, V. Teixeira, J. H. O. Nascimento, J. Neves, and P. B. Tavares, *J. Nanosci. Nanotechnol*., **11**, 1 (2011).
29. A. Buzarovska and A. Grozdanov, *J. Appl. Polym. Sci*., **123**, 2187 (2012).
30. Y. B. Luo, X. L. Wang, and Y. Z. Wang, *Polym. Degrad. Stab*., **97**, 721 (2012).
31. Z. Wanxi, Z. Chunxiao, and L. Hongji, *Nanoelectronics Conference*, INEC 2nd IEEE International, 24-27 March, 979 (2008).
32. J. G. Benito, E. Castillo, and J. F. Caldito, *Eur. Polym. J*., **49**, 1747 (2013).
33. H. Zhang, J. Huang, L. Yang, R. Chen, W. Zou, X. Lin, and J. Qu, *RSC Adv*., **5**, 4639 (2015).
34. N. V. Giang, T. Hoang, M. D. Huynh, T. H. Trung, D. V. Cong, V. M. Tuan, and T. D. Lam, *Adv. Sci. Lett*., **19**, 839 (2013).
35. A. K. Mohapatra, S. Mohanty, and S. K. Nayak, *Polym. Compos*., **33**, 2095 (2012).
36. J. Morshedian, P. M. Hoseinpour, H. Azizi, and R. Parvizzad, *Express Polym. Lett*., **3**, 105 (2009).
37. J. Zhao, M. Milanova, M. M. C. G. Warmoeskerken, and V. Dutschk, *Colloids Surf. A*, **413**, 273 (2012).
38. S. Varghese, J. Karger-Kocsis, and K. G. Gatos, *Polymer*, **44**, 3977 (2003).
39. N. Mohamad, A. Muchtar, M. J. Ghazali, D. H. Mohd, and C. H. Azhari, *Eur. J. Sci. Res*., **24**, 538 (2008).
40. A. Nalbandi, *Iran. Polym. J*., **10**, 371 (2001).
41. A. Marcilla, A. Gómez, and S. Menargues, *J. Anal. Appl. Pyrol*., **74**, 224 (2005).